of the Hydrolysis of COS," *Trans. Faraday Soc.*, 61, 681 (1965).
Thomas, W. J., and I. A. Furzer, "Diffusion Measurements in Liquid by the Gouy Method," *Chem. Eng. Sci.*, 17, 115 (1962).
van Krevelene, D. W., and P. J. Hoftijzer, "Sur la Solubilite des Gaz dans les Solutions Aqueuses," Chim. Ind. XXIme Congr. Int. Chim. Ind., Soc. Chim. Ind., Paris, p. 168 (1948).

Manuscript received August 3, 1978; revision received March 6, and accepted April 18, 1979.

The Effect of Gas and Solids Maldistribution on the Performance of Moving-bed Reactors: The Reduction of Iron Oxide Pellets with Hydrogen

JUN-ICHIRO YAGI
Research Institute of Mineral Dressing and Metallurgy
Tohoku University
1-1 Katahira 2-chome Sendai 980, Japan

and

JULIAN SZEKELY
Department of Materials Science and Engineering
Massachusetts Institute of Technology
Cambridge, Massachusetts 02139

A mathematical formulation is presented describing the reduction of iron oxide pellets with hydrogen in a counterflow moving-bed arrangement under conditions such that both the gaseous and the solids streams may be maldistributed. This maldistribution is imposed on the system by prescribing a radial variation in the void fraction and the particle size, together with a radial variation in the axial velocity of the solid stream.

In the formulation, allowance has been made for realistic chemical kinetics and nonisothermal behavior. Computer results are presented for both the maldistributed system and for base line cases where uniform gas and solids flow have been postulated.

It was found that maldistribution may play a very marked role in affecting the performance of the system, in particular, when the gas and the solid streams are mismatched, for example, preferential flow of gas near the walls and preferential flow of solids in the central core.

SCOPE

The countercurrent contacting of gaseous and solids streams in a packed-bed arrangement is of considerable practical interest in many materials processing operations (Yagi et al. 1968; Spitzer et al. 1968; Ishida and Wen 1971; Hara et al. 1976*a*, *b*). In the early work, it has been assumed that the axial velocity in the gaseous and solids streams was spatially uniform.

In recent work, Radestock and Jeschar (1970, 1971*a*, *b*), Stanek and Szekely (1972, 1973, 1974), and Szekely and Poveromo (1975) have shown that the postulate of spatially uniform velocity fields in packed beds may introduce serious errors. The effect of spatially nonuniform gas flows on the performance of moving packed-bed reactors has been studied very recently by Yagi and Szekely (1977*a*, *b*) and also by Kuwabara and Muchi (1976) who have shown that the overall conversion may indeed be affected quite markedly by the gas flow maldistribution. While these authors assumed a flat velocity profile for the solid stream, there are strong indications in the literature, notably due to the work of Chatlynne and Resnick (1973), Novosad and Surapati (1968), and Takahashi and Yanai (1973), that, in general, solids flow also tends to be maldistributed. In particular, for moving beds, the central portion of the solids would tend to move faster than the region close to the wall.

The purpose of this paper is to present a general formulation describing a reaction between a stream of particulate solids and a gas stream, contacted in a countercurrent moving-bed arrangement, under conditions that both the gaseous and the solid streams may be maldistributed. The particular system to be studied is the reaction between iron oxide pellets and hydrogen. The computed results will be compared with two sets of standard cases, corresponding to flat velocity profiles in both the gaseous and the solid streams and gas maldistribution with a flat solid velocity profile, respectively. As a result, a quantitative assessment will be presented of the part played by gas and solids flow maldistribution in affecting conversion in moving-bed reactors.

0001-1541-79-2710-0800-$01.35.

CONCLUSIONS AND SIGNIFICANCE

A mathematical formulation has been presented to describe the reaction of iron oxide pellets with hydrogen in a counterflow moving-bed arrangement, under conditions that both the gaseous and the solids streams are spatially nonuniform. The spatial nonuniformity of the gas stream was induced by imposing a particular radial distribution of porosity and particle size on the solid stream, while the radial distribution of the solid velocity was also prescribed. In the formulation, realistic kinetic expressions were used for representing the reaction rates; furthermore, allowance was made for nonisothermal behavior. The computed results presented indicate that maldistribution of the gaseous and solids streams may markedly affect the overall performance of the system, especially when the gaseous and the solid streams are mismatched.

Previous modeling work aimed at representing gas-solid reactions in moving-bed arrangements has neglected the effect of gas and solids flow maldistribution, with the exception of recent papers by Yagi and Szekely (1977*a*, *b*) and Kuwabara and Muchi (1976) who made allowance for nonuniform gas flow. The principal significance of the present paper is that it presents a general formulation describing the effect of gas and solids flow maldistribution on the performance of moving-bed reactors. Thus, the paper attempts to bring together information from the literature on chemical kinetics, nonuniform gas flow, and nonuniform solids flow.

Another potentially useful feature of the work is that it illustrates the application of these concepts on a system of considerable practical significance, namely, the reduction of iron oxides. In this process, the maldistribution is further complicated by the nonisothermality of the system and by the significant density change on the reaction by the gas.

Systems where a gas and a solid stream are contacted in a counterflow, moving-bed arrangement are of considerable practical importance in chemical reaction engineering. One particular example of interest is provided by the so-called direct reduction processes, where iron oxide pellets are reduced with a carbon monoxide hydrogen mixture (Tsay, Ray, and Szekely, 1976).

Over the years, a great deal of modeling work has been done to represent the behavior of these moving-bed systems (typical examples of which include papers by Yagi et al., 1968; Spitzer et al., 1968; Ishida and Wen, 1971; Hara et al., 1967*a*, 1976 *b*).

An important feature of these models is that in the statement of the problem, one has to combine information on the reaction of single particles with the flow conditions in the reactor.

The techniques for describing the reaction kinetics of single particles are reasonably well established, for example, Szekely, Evans, and Sohn (1976), but the representation of the flow behavior in these systems is somewhat more problematic.

In previous work aimed at the modeling of gas-solid reactions in moving-bed reactors, it has been generally assumed that the axial velocities in both the gaseous and the solid stream are uniform. Some allowance for departure from plug flow of the gas has, however, been made by considering axial and radial dispersion.

Recent work aimed at the characterization of the flow fields in packed-bed (and moving-bed) reactors has shown that the postulate of uniform velocity fields in the gaseous and the solids streams may introduce serious errors under certain circumstances. Nonuniform gas flow through packed beds has been studied by Radestock (1969), Radestock and Jeschar (1970, 1971*a*, *b*), Stanek and Szekely (1972, 1973, 1974), Szekely and Poveromo (1975), Szekely and Propster (1978), Araki (1976), and Araki and Moriyama (1977). Furthermore, the effect of nonuniform gas flows on the performance of moving-bed reactors has also received some attention, notably by Yagi and Szekely (1977*a*, *b*) and Kuwabara and Muchi (1976).

The flow pattern of solids in moving beds has been studied by a number of investigators, notably by Chatlynne and Resnick (1973), Novosad and Surapati (1968), and Takahashi and Yanai (1973). These authors have generally found that the postulate of a flat velocity profile would not be valid because in a moving bed the solids would tend to move faster in the central part of the column, while the region in the vicinity of the walls would tend to be retarded. It is generally appreciated that the actual flow pattern and distribution of the solids in moving-bed systems will depend on the charging arrangement, on the mode of withdrawal, and also on the system geometry, although these relationships have not been quantified.

Up to the present, no work has been done to relate the effect of nonuniform solids flow on the performance of moving-bed reaction systems.

Previous work by the present authors has shown that if the gas flow is maldistributed in a moving-bed reactor, this may have a profound effect on the performance of the system. The purpose of the present paper is to consider the more general case when both the gas flow and solids flow exhibit nonuniformities. The specific example to be studied is the reduction of iron oxides with a hydrogen stream, but it is expected that the general conclusions drawn should be rather more broadly valid regarding the behavior of moving-bed systems. Since the main purpose of the paper is to describe the effect of gas and solids flow maldistribution, the details of the actual rate expressions used for representing the reactions will not be discussed in the body of the paper but rather given in the appendix.

FORMULATION

Let us consider a two-dimensional moving bed in which spherical iron oxide pellets are being reduced (Figure 1). The solid pellets are charged at the top of the bed and move downward; the reducing gas is introduced at the bottom of the bed and ascends in a counterflow arrangement with the solid particles. The iron oxide pellets containing ferric oxide and magnetic iron oxide are reduced

to metallic iron through the intermediates magnetic iron oxide and ferrous oxide according to the chemical reactions shown below:

$$3Fe_2O_3 + H_2 = 2Fe_3O_4 + H_2O$$

$$Fe_3O_4 + H_2 = 3FeO + H_2O$$

$$FeO + H_2 = Fe + H_2O$$

Upon considering two-dimensional flow within a cylindrical coordinate system, we make the following assumptions:

1. Steady state.
2. Cylindrical symmetry.
3. Heat of reaction released to the solid particles.
4. Temperature distribution in a single particle is uniform.
5. Reaction rate of the individual iron oxide pellets is represented by the three-interface model of Hara et al. (1976).
6. The equation of motion for the gas is given by the Ergun Equations (5) and (6).
7. Radial distribution of the axial velocity of the solid particles is given.
8. Axial dispersion of heat and matter is neglected in the gas phase.

Within the framework of these assumptions, the governing equations have to express the conservation of the gaseous and the solid reactants, heat balance on the gas stream, heat balance on the solid stream, and the equation of motion for the gas stream. The additional relationships needed to specify the problem are the equation of continuity, that is, the overall mass balance, written for both the solid and the gas streams, and an appropriate kinetic expression for the reaction of the solids.

The dimensionless form of the governing equations may then be written as follows:

Mass balance on the hydrogen

$$-\alpha_1(P_e/P_o)(P/T_a)\frac{\partial^2 X_{H_2}}{\partial r^2} + \left[F_4 G_r - \alpha_1(P_e/P_o)(P/T_a) \times \left\{ \frac{1}{r} + \frac{2}{P}\frac{\partial P}{\partial r} - \frac{2}{T_a}\frac{\partial T_a}{\partial r} \right\} \right] \frac{\partial X_{H_2}}{\partial r} + F_4 \frac{R}{L} G_z \frac{\partial X_{H_2}}{\partial z} + \left(F_1 + X_{H_2}\frac{M_{H_2}}{M} F_2 \right) R^* - \alpha_1(P_e/P_o)(PX_{H_2}/T_a) \times \left[-\frac{1}{rT_a}\frac{\partial T_a}{\partial r} - \frac{1}{T_a}\frac{\partial^2 T_a}{\partial r^2} - \frac{2}{PT_a}\frac{\partial T_a}{\partial r}\frac{\partial P}{\partial r} + \frac{2}{T_a}\left(\frac{\partial T_a}{\partial r}\right)^2 + \frac{1}{rP}\frac{\partial P}{\partial r} + \frac{1}{P}\frac{\partial^2 P}{\partial r^2} \right] = 0 \quad (1)$$

Mass balance on the solid particles:

$$\frac{\partial G_{sz}}{\partial z} - \frac{L}{R}\frac{\partial}{\partial r}(rG_{sr}) - F_3 R^* = 0 \quad (2)$$

Heat balance on the gas:

$$\frac{R}{L} G_z \left\{ C_g \frac{\partial T}{\partial z} + T\frac{\partial C_g}{\partial z} \right\} + \left[G_r T \frac{\partial C_g}{\partial r} + \left\{ G_r C_g - \beta\left(\frac{\partial k_g}{\partial r} + \frac{k_g}{r} \right) \right\} \frac{\partial T}{\partial r} \right] - \beta k_g \frac{\partial^2 T}{\partial r^2} + \gamma(T - t) + F_2 C_g T R^* = 0 \quad (3)$$

where

$$\frac{\partial C_g}{\partial z} = \left[\Sigma X_i \left(\frac{dC_i'}{dT} \right) \left(\frac{\partial T}{\partial z} \right) + \Sigma (C_i' - C_g' M_i) \frac{\partial X_i}{\partial z} \right] C_{go} \Sigma M_i X_i$$

$$\frac{\partial C_g}{\partial r} = \left[\Sigma X_i \left(\frac{dC_i'}{dT} \right) \left(\frac{\partial T}{\partial r} \right) + \Sigma (C_i' - C_g' M_i) \frac{\partial X_i}{\partial r} \right] C_{go} \Sigma M_i X_i$$

Heat balance on the solid particles:

$$\left(\frac{R}{L}\right) \delta_s k_s \frac{\partial^2 t}{\partial z^2} + \beta_s k_s \frac{\partial^2 t}{\partial r^2} + \frac{R}{L} \left\{ G_{sz} \left(C_s \frac{\partial t}{\partial z} + t\frac{\partial C_s}{\partial z} + \delta_s \frac{\partial k_s}{\partial z}\frac{\partial t}{\partial z} \right\} + \left[-G_{sr} t \frac{\partial C_s}{\partial r} + \left\{ -G_{sr} C_s + \beta_s \times \left(\frac{\partial k_s}{\partial r} + \frac{k_s}{r} \right) \right\} \frac{\partial t}{\partial r} \right] + C_s t F_3 R^* + (-\Delta H)\zeta R^* + \gamma_s (T - t) = 0 \quad (4)$$

where

$$\frac{\partial C_s}{\partial z} = \left\{ \Sigma \frac{\partial G_{si}}{\partial z} (C_{si} - C_s) + \Sigma \frac{\partial C_{si}}{\partial z} G_{si} \right\} \Big/ \Sigma G_{si}$$

$$\frac{\partial C_s}{\partial r} = \left\{ \Sigma \frac{\partial G_{si}}{\partial r} (C_{si} - C_s) + \Sigma \frac{\partial C_{si}}{\partial r} G_{si} \right\} \Big/ \Sigma G_{si}$$

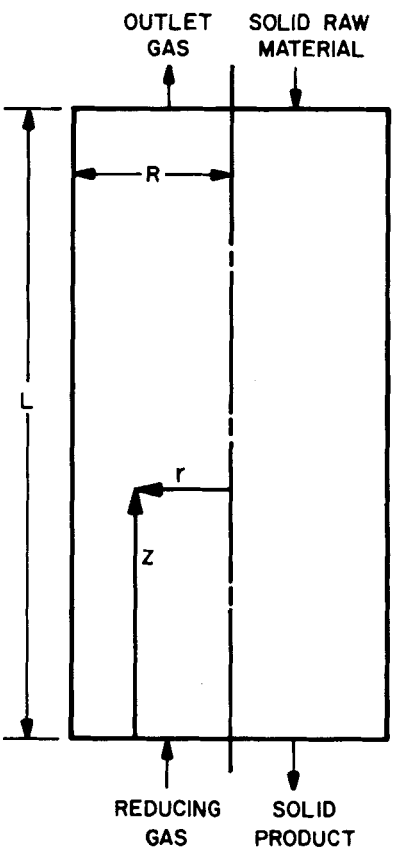

Fig. 1. Schematic diagram of a moving bed.

In order to determine the flow field of the gas, the Ergun equation is used to represent the equation of motion in the z and the r directions, respectively:

$$-\frac{\partial P}{\partial z} = f_1 G_z + f_2 G_z|G_z| \qquad (5)\dagger$$

$$-\frac{\partial P}{\partial r} = \frac{R}{L}(f_1 G_r + f_2 G_r|G_r|) \qquad (6)\dagger$$

The equation of continuity is given as follows for flow with a chemical reaction:

$$\frac{R}{L}\frac{\partial(rG_z)}{\partial z} + \frac{\partial}{\partial r}\left\{ rG_r - F_2\int_o^r R^* r dr \right\} = 0 \qquad (7)$$

It is convenient to recast Equations (5) and (6) in terms of the stream function; the manipulation is straightforward, available in the recent paper by Yagi and Szekely (1977*a*, *b*) and is not reproduced here.

RATE OF REACTION

When the overall rate is largely limited by pore diffusion, the reduction of hematite (ferric oxide) to metallic iron is thought to take place in three steps that occur at three distinct interfaces, as sketched in Figure 2.

The reaction rates, which implicitly entered into the formulation in the mass conservation equation, were represented, using a particular three-interface model, developed by Hara et al. (1976). The progressive advancement of the three reaction interfaces, namely, $Fe_2O_3/Fe_3O_4(X_1)$, $Fe_3O_4/FeO(X_2)$, and $FeO/Fe(X_3)$, may then be calculated from

$$\frac{dX_1}{dz} = \frac{L}{u_s}\frac{V_1}{4\pi r_o^3(X_1^2)(d_o/9)} \qquad (8)$$

$$\frac{dX_2}{dz} = \frac{L}{u_s}\frac{V_2}{4\pi r_o^3(X_2^2)(2d_o/9)} \qquad (9)$$

$$\frac{dX_3}{dz} = \frac{L}{u_s}\frac{V_3}{4\pi r_o^3(X_3^2)(2d_o/9)} \qquad (10)$$

The expressions for the overall rate of reaction R^* and the overall heat of reaction $(-H_T^o)$ are given below.

Overall reaction rate:

$$R^* = \frac{6(1-\epsilon_v)}{\pi d_P^3 \phi}(V_1 + V_2 + V_3)/R_o^* \qquad (11)$$

Overall heat of reaction:

$$(-\Delta H_T^o) = \frac{6(1-\epsilon_v)}{\pi d_P^3 \phi}\{(-\Delta H_T^o)_1 V_1 + (-\Delta H_T^o)_2 V_2 + (-\Delta H_T^o)_3 V_3\} \qquad (12)$$

The relationships describing the individual reaction steps, namely, V_1, V_2, and V_3, together with the relationships used for calculating the rate constants are given in the appendix.

† Ergun originally proposed the following equation as an empirical relationship between the pressure drop and the mass velocity.

$$\frac{\Delta P}{\Delta z} = f_1 G_z + f_2 G_z^2$$

Radestock (1969) pointed out that Equations (5) and (6) are not invariant to the transformation of the coordinates. However, Stanek and Szekely (1974) revealed that little error is introduced in using these equations in the case of largely parallel flow field; for this reason, in this paper, Equations (5) and (6) will be used as the equation of motion for gas.

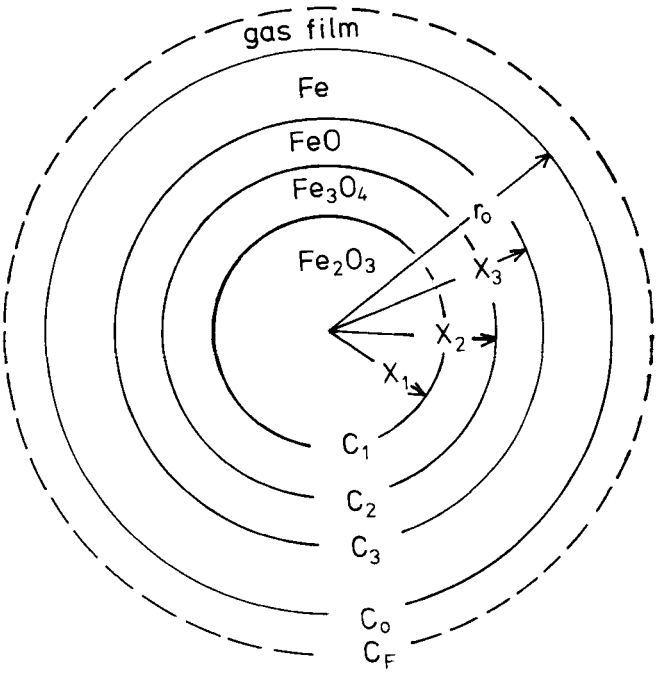

Fig. 2. Schematic representation of three-interface model.

BOUNDARY CONDITIONS

The boundary conditions required to complete the statement of the problem have to express the following constraints:

1. At the bottom of the bed ($z = 0$), the condition of the gas is specified.
2. At the top of the bed, the condition of the solid feed is specified.
3. Symmetry is observed at the center line.

Thus, we have

$$\left.\begin{aligned} G_z &= 1 \\ G_r &= 0 \\ X_{H_2} &= \text{const} \\ X_{H_2O} &= \text{const} \\ X_{N_2} &= \text{const} \\ \partial t/\partial z &= 0 \\ T &= 1 \\ P_o &= \text{const} \end{aligned}\right\} \text{at} \quad z = 0 \qquad (13)$$

X_{H_2}, X_{H_2O} and X_{N_2} are given from the operating conditions, but P_o has to be evaluated from the overall pressure drop and the top gas pressure.

The solid stream is charged, and gas stream is discharged at the top of the bed. The pressure field at the inlet is assumed to be uniform. The radial distribution of the axial velocity component of the solid stream was assumed to be parabolic function of r; furtherfore, the solid feed was assumed to contain no wustite or metallic iron.

Thus, the boundary conditions at the top of the bed are given as follows:

$$\left.\begin{aligned} &G_r = 0 \\ &\partial X_{H_2}/\partial z = 0 \\ &G_{sz} = f(r) \text{ to be specified} \\ &X_1 = 3\sqrt{1 - \left(\frac{55.85}{71.85}\right)\left(\frac{3C_{FeO}}{C_{Fe}}\right)} \\ &X_2 = 1 \\ &X_3 = 1 \\ &\partial T/\partial z = 0 \\ &P = 1 \\ &t = to/To \end{aligned}\right\} z = 1 \qquad (14)$$

TABLE 1. NUMERICAL VALUES OF THE OPERATING PARAMETERS

Length of the moving bed	10 m
Diameter of the bed	5 m
Apparent density of the pellet	4 120 kg/m^3 (solid)
Pressure of top gas	1 atm
Ambient temperature	20°C
Inlet solid temperature	20°C
Molar fraction of each component of inlet gas	$0.5(X_{H_2})$ $0.5(X_{N2})$

Symmetry at the central axis is expressed as

$$\left.\begin{array}{l} G_r = 0 \\ \partial X_{H_2}/\partial r = 0 \\ \partial t/\partial r = 0 \\ \partial T/\partial r = 0 \\ \partial P/\partial r = 0 \end{array}\right\} \text{at} \quad r = 0 \qquad (15)$$

The wall is impervious to gas; however, heat can be transferred through the wall. Thus, we have

$$\left.\begin{array}{l} G_r = 0 \\ \partial X_{H_2}/\partial r = 0 \\ -k_s\, \partial t/\partial r = (R/k_s^{\circ})h_{rs}(t - T_{am}) \\ -k_g\, \partial T/\partial r = (R/k_g^{\circ})h_r(T - T_{am}) \\ \partial P/\partial r = 0 \end{array}\right\} \text{at} \quad r = 1 \qquad (16)$$

METHOD OF SOLUTION

Equations (1) to (16), together with the appropriate subsidiary relationships, represent the complete statement of the problem. The governing equations were put in a finite-difference form and then were solved numerically. The successive overrelaxation method was employed for the solution of the second-order elliptic and parabolic equations, while simple difference equations were used to generate solutions for the first-order ordinary differential equations. Most of the calculations were carried out using a 101 × 11 grid, and the actual execution of the program required some 2 000 s, using a Cyber 173 digital computer.

The convergency criterion ϵ is defined as:

$$\sum_{\substack{i=1 \\ j=1}}^{\substack{j=J \\ i=I}} \left| \frac{Y_{l+1,i,j} - Y_{l,i,j}}{Y_{l,i,j}} \right| < \epsilon \qquad (17)$$

Here ϵ ranged from 0.02 to 0.0001, and Y is a dependent variable such as ψ, X_{H_2}, P, t, and T. Suffixes l, i, j designate the iteration number and the mesh points in the axial and the radial direction, respectively.

COMPUTED RESULTS

In the following we shall present a selection of the computed results, illustrating the effect of gas and solids flow maldistribution on the behavior of the system. The common property values used in the calculation are summarized in Table 1, while the particular cases of maldistribution examined are discussed in the following.

Variable Void Fraction and Particle Diameter

In general, gas flow maldistribution will occur if there is a spatial variation in the void fraction or in the diameter of the particles that make up the bed. In a physical sense, such nonuniformities may occur owing to the segregation of a charge (that is, caused by the feeding arrangements, or by the mode of removal) and or by the breakage of the particles. In real systems, the spatial

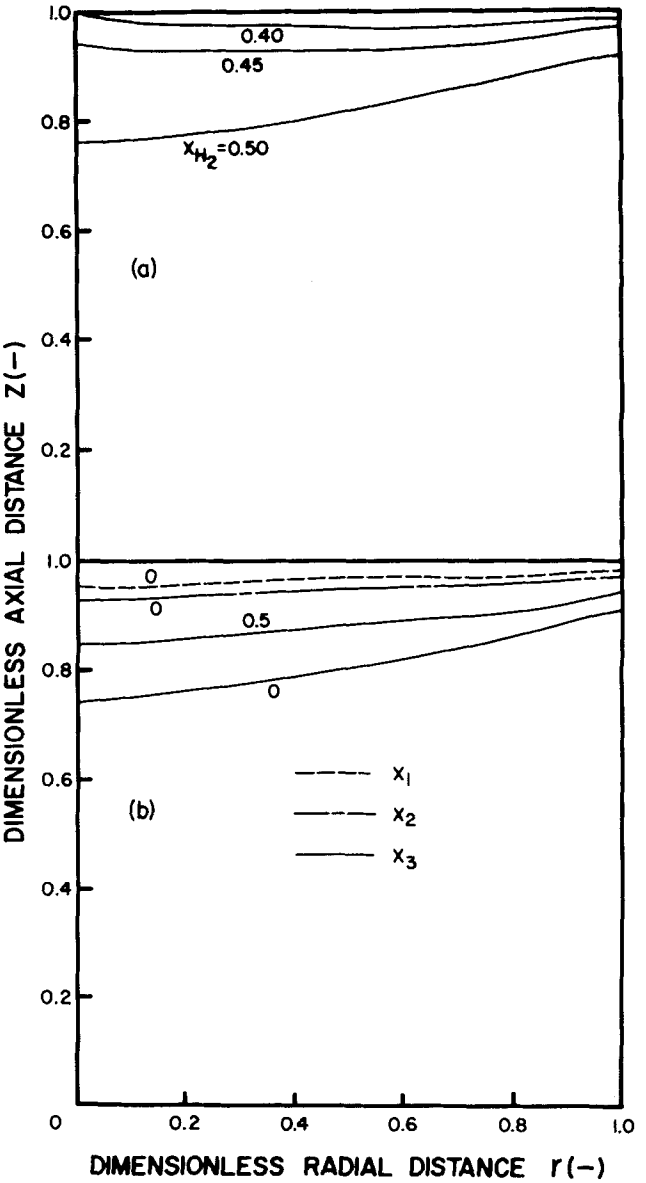

Fig. 3. Contour lines for X_{H_2}, X_1, X_2, and X_3 for $U_{max} = 3$, $T_0 = 900$, $G_0 = 9\,000$, and case A for d_p and ϵ_v.

distribution of the particle diameters and the fraction of voids may be a complex function which is affected by many of the process variables. However, in the absence of detailed information on real practical systems, we shall consider two idealized types of behavior, namely:

Case A: Loose packing at the center, larger particles at the center

$$\begin{aligned} \epsilon_v &= 0.45 - 0.1r; \qquad 0 < r < 1 \\ d_p &= 0.016 - 0.006r; \quad 0 < r < 1 \end{aligned} \qquad (18)$$

Case B: Dense packing at the center, larger particles at the wall

$$\begin{aligned} \epsilon_v &= 0.35 + 0.1r; \qquad 0 < r < 1 \\ d_p &= 0.01 + 0.006r; \quad 0 < r < 1 \end{aligned} \qquad (19)$$

Clearly, case A corresponds to a situation, where the resistance to gas flow increases radially as we progress from the center toward the wall, while the reverse is true for case B.

It follows that while both cases A and B are idealizations, they represent the broad class of problems where

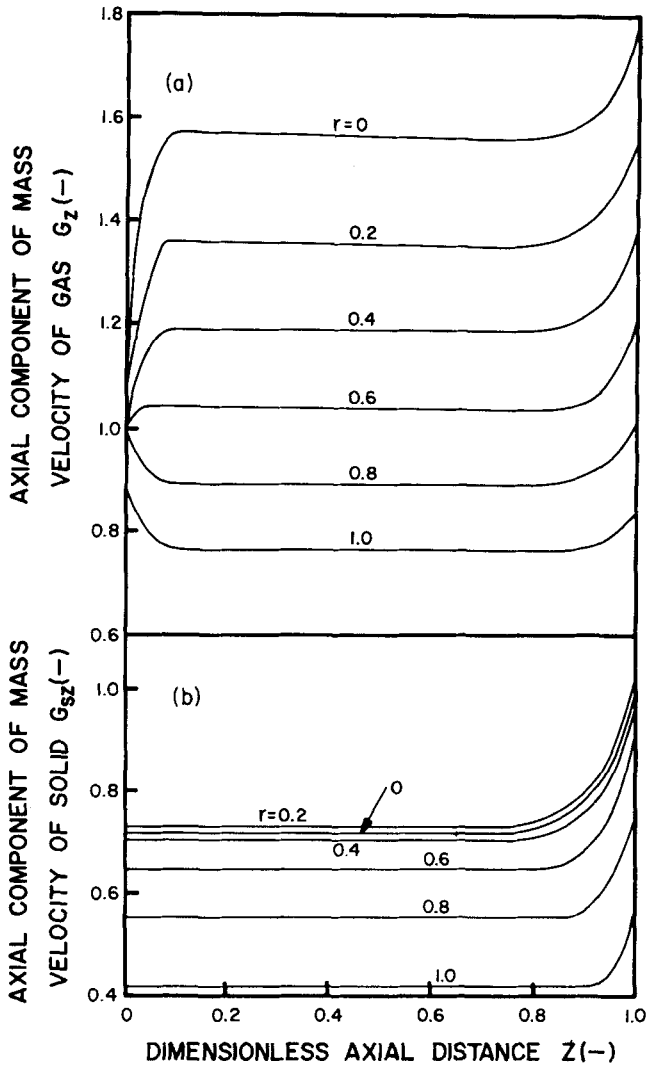

Fig. 4. Axial distributions of G_z and G_{sz} at various values of r for the same conditions as in Figure 3.

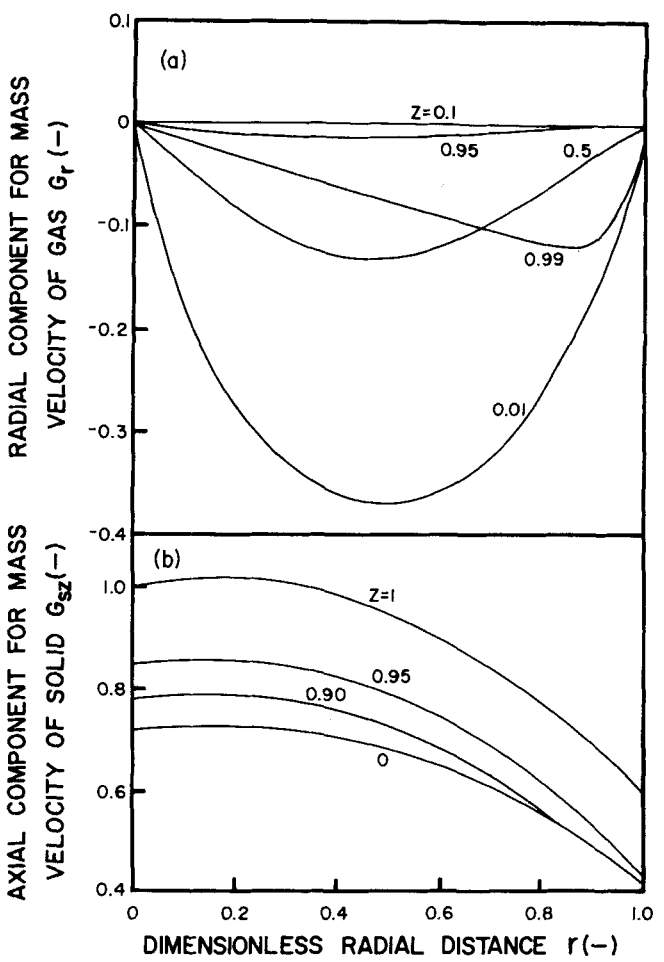

Fig. 5. Radial distributions of G_r and G_{sz} at various values of z for the same conditions as in Figure 3.

there is preferential flow of the gas in the central core and in the vicinity of the walls, respectively.

It has to be stressed that these structural considerations pertaining to gas flow maldistribution will be necessarily modified by the development of the reaction fronts and the changes of gas composition and gas temperatures. These effects will be discussed during the presentation of the results.

Solids Flow

The mass velocity of the solids at the entrance is given by the following expression:

$$G_{szo} = U_s \rho_a (1 - \epsilon_v) \tag{20}$$

In previous publications, U_s was assumed to be constant; however, there is strong evidence that, in general, U_s may depend on the radial position within the bed. The exact nature of this relationship is not known at this time, but it is reasonable to suppose that under many circumstances U_s will tend to decrease as we proceed radially toward the wall. In the absence of a predictive relationship for $U_s = f(r)$, as a first approximation let us postulate

$$U_s = U_{\max}\left(1 - \frac{r^2}{2}\right) \tag{21}$$

which allows for cylindrical symmetry and a radially decreasing solids velocity.

Figures 3, 4, and 5 show the computed results for case A for a gas inlet temperature of 900°C. Figure 3 shows the maps of the gas mole fraction isopleths together with the positions of the reaction fronts. Figure 4 shows the maps of the axial profiles for the gas and solids mass velocity components, while the radial profiles of the radial gas velocity and the axial solids velocity are given in Figure 5. We note that the axial mass velocity of the solid stream varies both because of the solids flow profile imposed on the system and owing to the gradual conversion of the solids, which involves a reduction in the apparent solid density.

It is of interest to contrast Figure 3 with Figure 6, which has been computed for a uniform solids flow. It is seen that the concentration and reaction front isopleths are much more distorted in the latter case. This behavior is readily explained by considering the fact that for the geometry considered and for case A, there is preferential gas flow in the central core of the bed. In case of Figure 3 (allowing for nonuniform solids flow), this preferential gas flow in the central core is matched by a compensating preferential solid flow in the central region, resulting in relatively uniform concentration isopleths. This compensating effect is absent for the case depicted in Figure 6.

It is of interest to compare Figures 3 and 6 with Figure 7, which has been computed for case A also but for a spatially uniform gas flow, corresponding to the mean values of the porosity and particle diameter in the bed.

As before, the mass velocity of the solids at the entrance is given by Equations (20) and (18), but in this case a constant value has been taken for U_s.

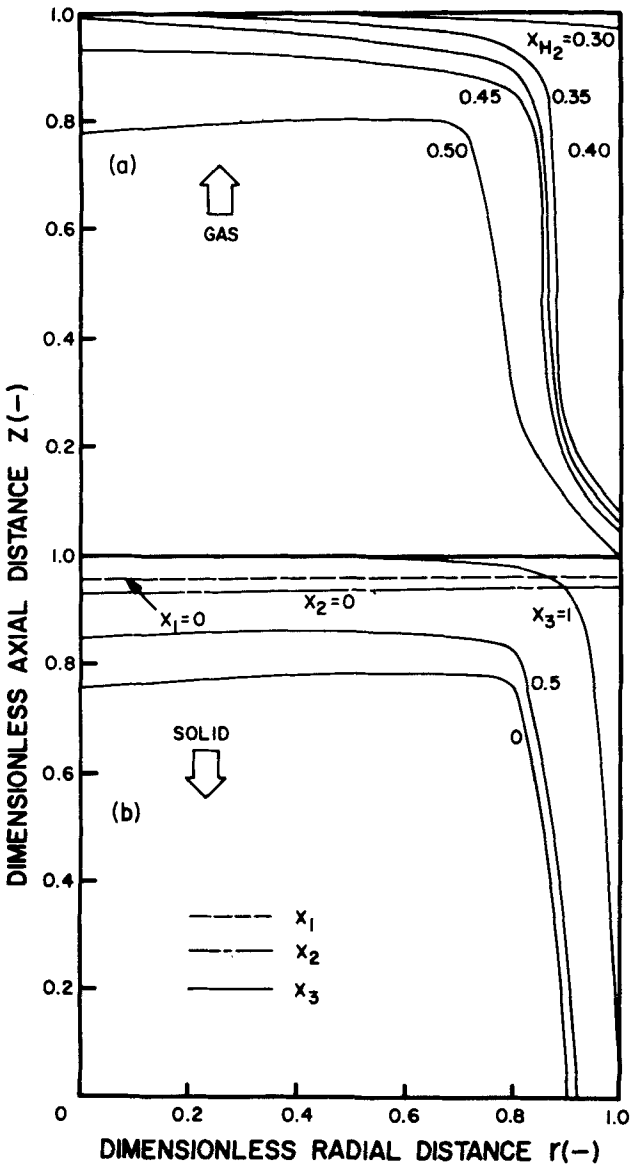

Fig. 6. Contour lines for X_{H_2}, X_1, X_2, and X_3 for the same conditions as in Figure 3, but $u_s = 3$ (constant).

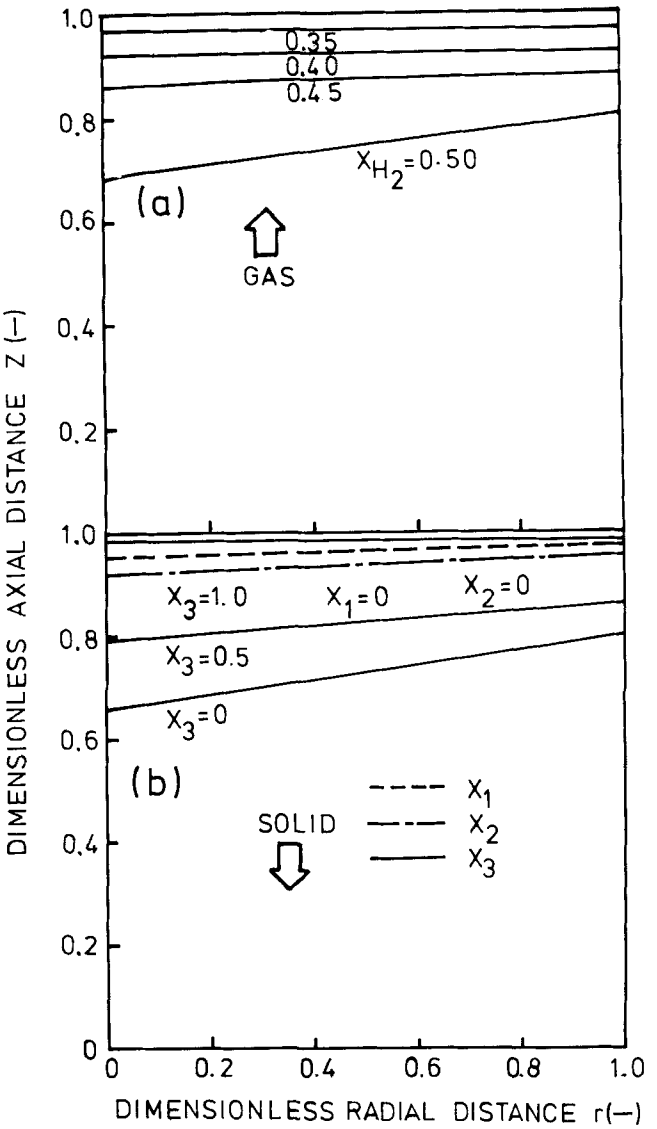

Fig. 7. Contour lines for X_{H_2}, X_1, X_2, and X_3 for $U_s = 3$, $T_0 = 900$, $G_0 = 9\,000$, and case A for d_p and ε_v. (Uniform gas and solid flow.)

As expected, Figure 7 depicts relatively uniform concentration isopleths; the small radial distribution found is attributable to the variations in void fraction, the effect of which has been retained in representing the solids flow.

Figures 8, 9, and 10 give the profiles corresponding to the cases depicted in the previous Figures 3, 4, and 5, respectively, but for case B, where the void fraction and particle size distribution would provide for preferential gas flow near the walls.

It is seen that under these conditions, the concentration isopleths are markedly distorted because of the mismatch between the gas and the solids flows, namely, preferential gas flow near the walls and preferential solids flow in the central core.

Figure 11 shows the computed isopleths for case A but for an inlet gas temperature of 800°C. Because of the kinetic parameters chosen, this lower inlet gas temperature causes chemical kinetics to play a larger role in determining the overall rate of reaction. For this reason, the system appears to be more sensitive to flow maldistribution than found for the higher inlet gas temperature; this behavior is readily seen on comparing Figures 3 and 11, where the latter shows a rather more marked distortion of the concentration and reaction front isopleths.

DISCUSSION

A formulation has been developed, and computed results are presented, describing the reduction of hematite with hydrogen in a counterflow moving-bed arrangement under conditions such that both the gaseous and the solid streams may be maldistributed. This reaction system was chosen because the reaction kinetics are well understood, and it is of considerable practical importance. Furthermore, over the temperature range studied, the effect of both diffusion and chemical kinetics control could be explored.

The maldistribution of the gas was produced by imposing particular radial distributions of the porosity and particle size forming the moving bed, which resulted in a spatially variable resistance to flow.

Two specific cases were considered, namely, case A where the void fraction and the average particle size decreased from the center of the column toward the wall and case B where the reverse was true. It follows that case A results in preferential flow through the central

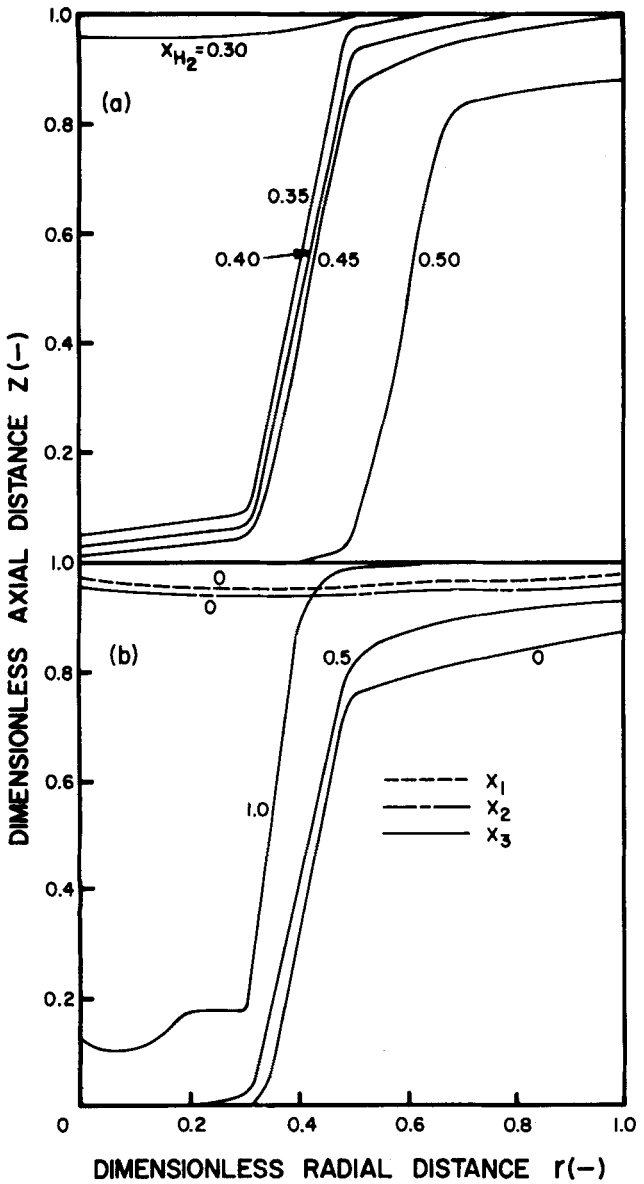

Fig. 8. Contour lines for X_{H_2}, X_1, X_2, and X_3 for $U_{max} = 3$, $T_0 = 900$, $G_0 = 9\,000$, and Case B for d_p and ε_v.

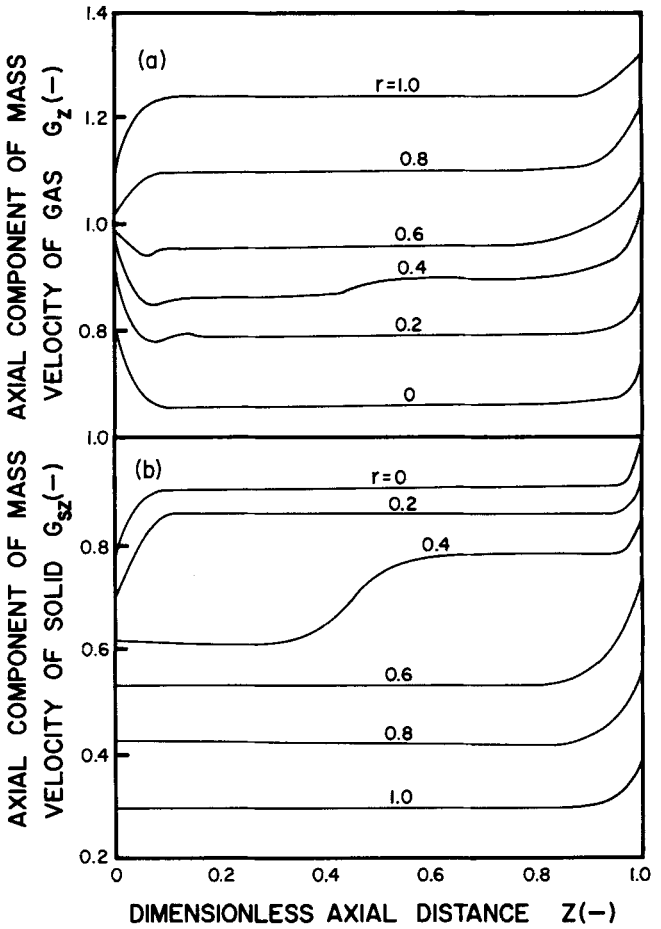

Fig. 9. Axial distributions of G_z and G_{sz} at various values of r for the same conditions as in Figure 8.

core of the column, while case B produces preferential flow of the gas in the peripheral region of the bed.

The spatially nonuniform solids flow results in part from the variable porosity and in part from the parabolic vertical velocity component specified for the solid stream.

A comment should be made regarding the physical basis for the types of maldistribution that have been considered in the paper. The formulation has been developed in quite a general way, and the computational techniques employed would have been capable of handling almost any arbitrary spatially distributed flow resistance and solids flow distribution.

Ideally, one should have used experimentally determined distributed gas flow resistance and solid velocities, but unfortunately no such information is available at present on real, operating systems that could be put in an appropriate quantitative form.

Regarding the operation of countercurrent moving-bed systems, studies have been made on the charge distribution in iron blast furnaces, and it has been found that a broad range of distribution arrangements is possible, depending on the system geometry (Sstandish, 1977). Of the two cases considered in the paper, namely A and B, case B could be more readily visualized for systems where a solid charge containing a range of particle sizes is introduced in the vicinity of the axis of the bed. Under these conditions, the larger particles would tend to migrate toward the wall, while the central core would contain a more densely packed mixture of larger and finer particles.

The alternative arrangement, cases A and B considered in the paper, together with the base line case of uniform gas and solids flow, is thought to represent a broad range of conditions that one may encounter in practice.

The important finding reported in the paper is that gas and solid flow maldistribution may have a major deleterious effect on the performance of moving-bed reactors. These effects have been expressed in a quantitative manner for the specific case of iron oxide reduction with hydrogen, but it is thought that at least in a qualitative sense these results have rather broader implications.

Spatially nonuniform gas and solids flows will occur when the distribution of the particle sizes and the void fraction of the bed are spatially nonuniform. In general, one may consider two groups of cases, in addition to the studies case where the flow of both streams is uniform.

One system, exemplified by case A, would correspond to a case where the resistance to gas flow is the lowest in the center and increases radially outward, while the solids flow decreases as we move from the center toward the wall. Under these conditions, the two maldistributed streams may partially or fully compensate each other, resulting in relatively flat concentration isopleths.

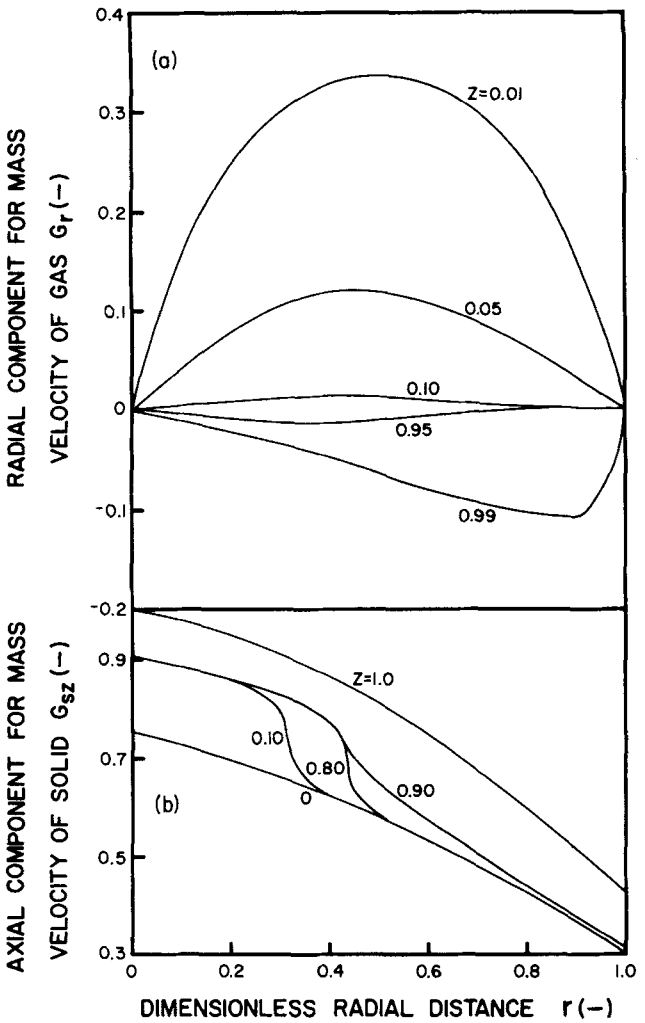

Fig. 10. Radial distributions of G_r and G_{sz} at various values of z for the same conditions as in Figure 8.

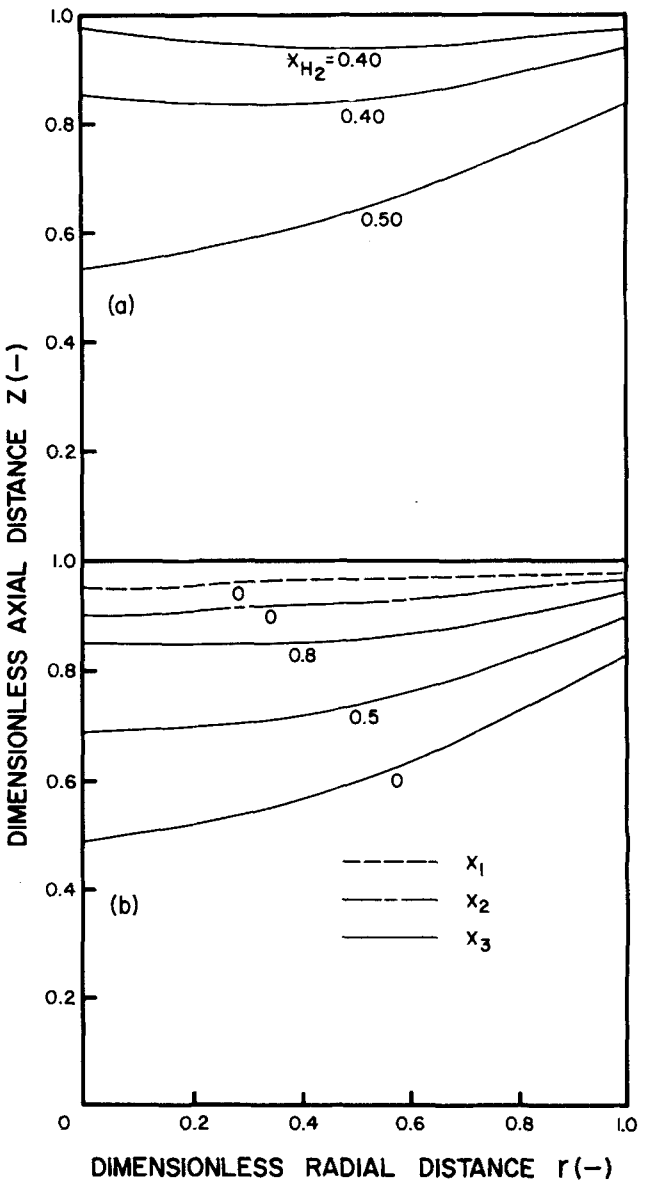

Fig. 11. Contour lines for X_{H_2}, X_1, X_2, and Z_3 for $U_{max} = 3$, $T_0 = 800$, $G_0 = 9\,000$, and case A for d_p and ϵ_v.

It is thought, however, that in many instances it would be more realistic physically, to consider the converse situation, illustrated by case B. Under these conditions, the resistance to flow increases as we progress from the wall toward the center, while the velocity of the solids is at a maximum in the center of the column. In such a case, a severe mismatch of the two streams may occur, resulting in very poor utilization of the reactor volume. As shown, these problems would be even more aggravated if the system were to operate in the regime where the overall rate is controlled by chemical kinetics, because under these conditions there is an even greater sensitivity to the concentration of the reducing gas in the region of diffusion or mass transfer control.

The principal conclusion that may be drawn from this work is that the maldistribution of gaseous and solids streams, which is known to occur in the operation of moving-bed reactors, may have a very marked role in affecting the performance of the system. Scale-up from laboratory to full scale units, changes in solids feed consistency, and alterations in the feeding arrangements of the gaseous and the solid streams may all have an important effect in modifying the spatial distribution. The formulation presented in the paper illustrated this behavior for a particular system but also provided a general frame work for the analysis of a broad class of problems.

It would be desirable to combine the analysis presented here with realistic, measured data, concerning the velocity distribution of solids and the spatial dependence of particle sizes and void fractions in moving bed systems. However such information is not available at present. It is hoped that by drawing attention to the important role of solids gas flow maldistribution in determining the performance of packed bed reactors, work will be stimulated in this area.

NOTATION

C_{Fe} = total iron content of iron oxide pellet
C_{FeO} = ferrous oxide content of iron oxide pellet
C_o = molar density of gas at inlet condition (kgmole/m^3)
C_F = molar concentration of reducing gas (hydrogen) in bulk (kgmole/m^3)
C_1, C_2, C_3 = molar concentration of reducing gas at the reaction interfaces of ferric oxide/magnetic iron oxide, magnetic nonoxide/ferrous oxide, and ferrous oxide/iron (kgmole/m^3)
C_{e1}, C_{e2}, C_{e3} = equilibrium concentration of gas for the reaction of ferric oxide/magnetic iron oxide, magnetic nonoxide/ferrous oxide, and ferrous oxide/iron (kgmole/m^3)

C_g, C_g' = specific heat of gas mixture, dimensionless and dimensional (kcal/kg·°C)
C_i, C_i' = molar specific heat of gas species i, dimensionless and dimensional [kcal/kgmole(i)·°C]
C_{go} = $(X_iC_i)_o/(M_iX_i)_o$(kcal/kg·°C)
C_s = dimensionless specific heat of solid pellet
C_{si} = specific heat of solid species i (kcal/kg·°C)
C_{so} = specific heat of solid pellet at inlet condition (kcal/kg·°C)
D_{H_2} = effective diffusivity of reducing gas in the reactor (m²/hr)
D_H = molecular diffusion coefficient of hydrogen in gas mixture (m²/hr)
D_{e1}, D_{e2}, D_{e3} = effective diffusivity of reducing gas in the porous magnetic iron oxide, ferrous oxide, and iron (m²/hr)
d_p = diameter of a pellet (m)
d_o = initial content of reducing oxygen atom in the pellet [kgatom(0)/m³(solid)]
F_1, F_2, F_3 = $RM_{H_2}R_o^*/G_o$, $M_{O_2}RR_o^*/2G_o$, and $M_{O_2}LR_o^*/2G_{so}$
F_4 = $M_{H_2}M_{H2O} + X_{N_2}(M_{N_2} - M_{H2O})/\overline{M}^2$
f_1, f_2 = $150(1-\epsilon_v)^2\mu_{mix}LG_o/(g_c\epsilon_v^3d_p^2\phi\rho P_e)$, $1.75(1-\epsilon_v)LG_o^2/(g_cd_p\phi\epsilon_v^3P_e)$
G_r, G_z = radial and axial dimensionless mass velocity of gas
G_o = mass velocity of gas at inlet condition (kg/m²·hr)
G_{sr}, G_{sz} = radial and axial dimensionless mass velocity of iron oxide pellets
G_{szo} = mass velocity of iron oxide pellets at the top of the reactor (kg/m²·hr)
G_{si} = mass velocity of solid species i (kg/m²·hr)
g_c = conversion coefficient for gravity (kg·m/kg·m²)
$(-\Delta H_T^o)_i$, $(-\Delta H)$ = heat of reaction for i^{th} chemical reaction and dimensionless overall heat of reaction [kcal/kgmole(H_2)]
h_p = convective heat transfer coefficient between gas and solid particle (kcal/m²·hr·C)
h_r = heat transfer coefficient from the gas stream to the reactor wall (kcal/m²·hr·C)
h_{rs} = heat transfer coefficient from the solid stream to the reactor wall (kcal/m²·hr·C)
h_{rv} = radiant heat transfer coefficient (kcal/m²·hr·C)
K_1, K_2, K_3 = equilibrium constants of the chemical reaction from ferric oxide to magnetic iron oxide, magnetic iron oxide to ferrous oxide, and ferrous oxide to iron
k_1, k_2, k_3 = reaction rate constants of chemical reactions from ferric oxide to magnetic iron oxide, magnetic iron oxide to iron, and ferrous oxide to iron (m/hr)
k_f = mass transfer coefficient around the pellet (m/hr)
k_F = thermal conductivity of gas mixture (kcal/m·hr·C)
k_g, k_g', k_g^o = effective thermal conductivity of gas, dimensionless, dimensional and at the inlet condition kcal/m·hr·C)
k_s, k_s', k_s^o = effective thermal conductivity of solid pellets, dimensionless, dimensional and at the inlet condition (kcal/m·hr·C)
L = axial length of reactor (m)
M_i = molar weight of gas species i (kg/kgmole)
$\overline{M}$ = average molar weight of gas (kg/kgmole)
P, P_e, P_o = pressure of gas, dimensionless, at outlet and at inlet condition (kg/m²)
Pr = Prandtl number
R = radius of reactor (m)
R^*, R_o^* = dimensionless overall reaction rate and overall reaction rate at inlet condition [kgmole(H_2)/m³(bed)·hr]
r = dimensionless radial distance from the center in the reactor
r_o = radius of the pellet (m)
Re_p = Reynolds number
Sh = Sherwood number
Sc = Schmidt number
T, T', T_o = gas temperature, dimensionless, dimensional and at inlet condition (°C)
T_a = dimensionless gas temperature $(T' + 273)/(T_o + 273)$
T_{am} = dimensionless ambient temperature
t, t', t_o = solid temperature, dimensionless, dimensional and at inlet condition (°C)
U_{max} = maximum velocity of solid in axial direction (m/hr)
U_s = axial velocity of solid (m/hr)
V_1, V_2, V_3 = reaction rate from ferric oxide to magnetic iron oxide, magnetic iron oxide to ferrous oxide, and ferrous oxide to iron [kgmole(H_2)/hr particle]
X_1, X_2, X_3 = dimensionless radial distance of reaction interface from the center of the pellet
X_i = molar fraction of gas species i
z = dimensionless axial distance from the bottom of the reactor

Greek Letters

α_1, α_2 = $M_{H_2}D_{H_2r}C_o/G_oR$, $M_{H_2z}C_o/G_oR$
β, β_s = k_g^o/RG_oC_{go}, $k_s^o/C_{so}G_{so}R$
γ, γ_s = $6(1-\epsilon_v)h_pR/G_oC_{go}d_p\phi$, $6(1-\epsilon_v)h_pR/C_sG_{so}d_p\phi$
δ, δ_s = $k_g^o/C_{go}G_oL$, $k_s^o/C_{so}G_s^oL$
ϵ_v = voidage in the reactor
ζ = $RR_o^*(-H^\circ_{298})/C_{so}d_p\phi$
μ_{mix} = viscosity of gas mixture (kg/m·hr)
ρ = density of gas (kg/m³)
ρ_a = apparent density of solid pellet [kg/m³(solid)]
ϕ = shape factor
ψ = stream function

APPENDIX: DEFINITION OF THE RATE EXPRESSIONS AND RATE CONSTANTS

Rate Expressions for the Interfacial Reaction

The rate of the individual chemical reactions given by

$$V_1 = 4\pi r_o^2[\{A_3(A_2 + B_2 + B_3 + F) + (A_2 + B_2)(B_3 + F)\}(C_F - C_{e1}) - (B_4 + F)A_2(C_F - C_{e3}) - \{A_3(B_2 + B_3 + F) + B_2(B_3 + F)\} \times (C_F - C_{e2})]/W_1 \quad (A1)$$

$$V_2 = 4\pi r_o^2[\{(A_1 + B_1 + B_2)(A_3 + B_3 + F) + A_3(B_3 + F)\} \times (C_F - C_{e2}) - \{B_2(A_3 + B_3 + F) + A_3(B_3 + F)\} \times (C_F - C_{e1}) - (A_1 + B_1)(B_3 + F)(C_F - C_{e3})]/W_1 \quad (A2)$$

$$V_3 = 4\pi r_o^2[\{(A_1 + B_1)(A_2 + B_2 + B_3 + F) + A_2 \times (B_2 + B_3 + F)\}(C_F - C_{e3}) - A_2(B_3 + F) \times (C_F - C_{e1}) - (A_1 + B_1)(B_3 + F)(C_F - C_{e2})]/W_1 \quad (A3)$$

where

$$W_1 = (A_1 + B_1)\{A_3(A_2 + B_2 + B_3 + F) + (A_2 + B_2) \times (B_3 + F)\} + A_2\{A_3(B_2 + B_3 + F) + B_2(B_3 + F)\}$$

After the reaction V_1 is completed, two reaction interfaces remain between magnetic iron oxide and ferrous oxide, and ferrous oxide and iron. At this stage we have

$$V_1 = 0 \quad \text{(A4)}$$

$$V_2 = 4\pi r_o^2[(A_3 + B_3 + F)(C_F - C_{e2}) - (B_3 + F)(C_F - C_{e3})]/W_2 \quad \text{(A5)}$$

$$V_3 = 4\pi r_o^2[(A_2 + B_2 + B_3 + F)(C_F - C_{e2}) - (B_3 + F)(C_F - C_{e2})]/W_2 \quad \text{(A6)}$$

where

$$W_2 = (A_2 + B_2)(A_3 + B_3 + F) + A_3(B_3 + F)$$

Finally, when reactions V_1 and V_2 are completed, only one reaction interface remains between ferrous oxide and iron. At this stage we have

$$V_1 = 0 \quad \text{(A7)}$$

$$V_2 = 0 \quad \text{(A8)}$$

$$V_3 = 4\pi r_o^2(C_F - C_{e3})/W_3 \quad \text{(A9)}$$

where

$$W_3 = A_3 + B_3 + F$$

$$A_1 = 1/X_1^2k_1(1 + 1/K_1), \quad A_2 = 1/X_2^2k_2(1 + 1/K_2)$$

$$A_3 = 1/X_3^2k_3(1 + 1/K_3), \quad B_1 = (X_2 - X_1)r_o/D_{e1}X_1X_2$$

$$B_2 = (X_3 - X_2)r_o/D_{e2}X_2X_3, \quad B_3 = (1 - X_3)r_o/D_{e3}X_3$$

$$F = 1/k_f$$

Rate Constants, Equilibrium Constant and Heat of Reaction

Rate constants and equilibrium constants used in the reaction model were taken from Hara et al. (1974). These expressions take the following forms:

$$k_1 = 1.44 \times 10^5 \exp\{-6\,650/(t' + 273)\} \quad \text{(A10)}$$

$$k_2 = 2.88 \times 10^5 \exp\{-8\,000/(t' + 273)\} \quad \text{(A11)}$$

$$k_3 = 2.45 \times 10^7 \exp\{-1\,400/(t' + 273)\} \quad \text{(A12)}$$

The effective diffusivity of hydrogen through the porous intermediate solid phases was estimated from

$$D_{e1} = 0.13D_H \quad \text{(A13)}$$

$$D_{e2} = 0.20D_H \quad \text{(A14)}$$

$$D_{e3} = 0.35D_H \quad \text{(A15)}$$

The pore diffusion coefficients depend on the solid structure. The numerical values selected were quoted from Hara's work (1974).

The equilibrim constants are given as

$$K_1 = \exp\{362/(t' + 273) + 10.32\} \quad \text{(A16)}$$

$$K_2 = \exp\{-8\,580/(t' + 273) + 8.98\} \quad \text{(A17)}$$

$$K_3 = \exp\{-2\,070/(t' + 273) + 1.30\} \quad \text{(A18)}$$

The equations for the heat of reaction were derived from the data given by von Bogdandy and Engell (1971):

$$\begin{aligned}(\simeq\Delta H_T^o)_1 &= 2.60\,t' + 2\,220 && 100 < t' < 300°C\\ &= 3\,000 && 300 < t' < 800°C\\ &= 3.61\,t' + 112 && 800 < t' < 1\,300°C\end{aligned} \quad \text{(A19)}$$

$$\begin{aligned}(-\Delta H_T^o)_2 &= 10.37\,t' - 21\,090 && 100 < t' < 911°C\\ &= -11.640 && 911 \leq t' < 1\,300°C\end{aligned} \quad \text{(A20)}$$

$$\begin{aligned}(-\Delta H_T^o)_3 &= 3.88\,t' - 5\,810 && 100 \leq 500°C\\ &= 3\,870 && 500 \leq t' \leq 927°C\\ &= 3.37\,t' - 6\,990 && 927 \leq t' \leq 1\,300°C\end{aligned} \quad \text{(A21)}$$

LITERATURE CITED

Araki, K., "Gas Flow Patterns and Pressure Profiles in Non-Uniform Packed Beds," *Tetsu-to-Hagane*, **62**, 1485 (1976).

———, and A. Moriyama, "Gas Flow through Packed and Moving Beds with Layered Burdens," *ibid.*, **63**, 1453 (1977).

Chatlynne, C. J., and W. Resnick, "Determination of Flow Patterns for Unsteady-State Flow of Granular Materials," *Powder Technol.*, **8**, 177 (1973).

Hara, Y., M. Sakawa, and S. Kondo, "Mathematical Model of the Shaft Furnace for Reduction of Iron-Ore Pellet," *Tetsu-to-Hagane*, **62**, 315 (1976*a*).

———, "Analysis of Operating Conditions of Shaft Furnace for Reduction of Iron-Ore Pellet by Using a Mathematical Model," *ibid.*, 324 (1976*b*).

Ishida, M., and C. Y. Wen, "Analysis of Nonisothermal Moving Bed for Noncatalytic Solid-Gas Reactions," *Ind. Eng. Chem. Process Design Develop.*, **10**, 164 (1971).

Kuwabara, M., and I. Muchi, "Theoretical Analysis of Gas Flow in Shaft with Layered Burdens," *Tetsu-to-Hagane*, **62**, 463 (1976).

Novosad, J., and K. Surapati, "Flow of Granular Materials: Determination and Interpretation of Flow Patterns," *Powder Technol.*, **2**, 82 (1968/69).

Radestock, J., "Theoretische Untersuchung der Stationaeren Inkompressiblen und Kompressiblen Stroemung in Ruhenden, Geschichteten und Isotropen Schuettunger," Dissertation, Fakult, Bergbau, Huettenwesen and Masschin. Techn. Univ. Clausthal (1969).

———, and R. Jeschar, "Ueber die Stroemung durch die Hochofenschuettung," *Stahl Eisen*, **22**, 1249 (1970).

———, "Theoretishe Untersuchung der Inkompressiblen und Kompressiblen Stroemung durch Reaktor-Schuettungen," *Chem. Ing. Tech.*, **43**, 355 (1971*a*).

———, "Theoretishe Untersuchung der Gegenseitigen Beeinflussung von Temperature and Stroemungsfeldern in Schuettunger," *ibid.*, **43**, 1304 (1971*b*).

Spitzer, R. H., F. S. Manning, and W. O. Philbrook, "Simulation of Topochemical Reduction of Hematite via Intermediate Oxide in an Isothermal Counter-current Reactor," *Trans. Met. Soc. AIME*, **242**, 618 (1968).

Standish, N. T., *Blast Furnace Aerodynamics*, Wollongond, Australia (1977).

Stanek, V., and J. Szekely, "The Effect of Non-uniform Porosity in Causing Flow-Maldistribution in Isotherman Packed Bed," *Can. J. Chem. Eng.*, **50**, 9 (1972).

———, "Flow Maldistribution in Two-Dimensional Packed Beds Part II: The Behavior of Non-isothermal System," *ibid.*, **51**, 22 (1973).

———, "Three Dimensional Flow of Fluid Through Non-uniform Packed Beds," *AIChE J.*, **20**, 974 (1974).

Szekely, J., and J. J. Poveromo, "Flow Maldistribution in Packed Beds: A Comparison of Measurements with Predictions," *ibid.*, **21**, 769 (1975).

———, and M. A. Propster, "Resistance of Layer-Charged Blast Furnace Burdens to Gas Flow," *Ironmaking & Steelmaking*, **4**, 15 (1977).

———, J. W. Evans, and H. Y. Sohn, *Gas-Solid Reactions*, Academic Press, New York (1976).

Takahashi, H., and H. Yanai, "Flow Profile and Void Fraction of Granular Solids in a Moving Bed," *Powder Technol.*, **7**, 205 (1973).

Tsay, Q. T., W. H. Ray, and J. Szekely, "The Modeling of Hematite Reduction with Hydrogen Plus Carbon Monoxide Mixture," *AIChE J.*, **22**, 1064 (1976).

Von Bogdandy, L., and H. J. Engell, *The Reduction of Iron Ores*, Springer-Verlag, Berlin, Germany (1971).

Yagi, J., A. Moriyama, and I. Muchi, "Theoretical Analysis on the Reduction of Iron-oxide Pellets in Isothermal Moving Bed," *J. Japan Inst. Metals*, **32**, 209 (1968).

———, and J. Szekely, "A Mathematical Formulation for the Reduction of Iron Oxide Pellets in Moving Beds with Non-uniform Gas and Solids Flow," *Trans. Iron & Steel Inst. Japan*, **17**, 569 (1977*a*).

———, "Computed Results for the Reduction of Iron Oxide Pellets in Moving Beds with Non-uniform Gas and Solids Flow," *ibid.*, **17**, 576 (1977*b*).

Manuscript received January 3, 1978; revision received October 3, 1978, and accepted March 23, 1979.